sciendo

CAIM
ISSN 2038-0909

Commun. Appl. Ind. Math. 10 (1), 2019, 182–198 DOI: 10.1515/caim-2019-0020

Research Article

Application of Energetic BEM to 2D Elastodynamic Soft Scattering Problems

A. Aimi[1§*], L. Desiderio[2§], M. Diligenti[1§], C. Guardasoni[1§]

[1]Department of Mathematical, Physical and Computer Sciences, University of Parma, Italy

[2]Department of Mathematical Sciences, Politecnico di Torino, Italy

[§]Members of the INDAM-GNCS Research Group, Italy

[*]Email address for correspondence: alessandra.aimi@unipr.it

Communicated by Giovanni Russo

Received on 10 22, 2018. Accepted on 09 13, 2019.

Abstract

Starting from a recently developed energetic space-time weak formulation of the Boundary Integral Equations related to scalar wave propagation problems, in this paper we focus for the first time on the $2D$ elastodynamic extension of the above wave propagation analysis. In particular, we consider elastodynamic scattering problems by open arcs, with vanishing initial and Dirichlet boundary conditions and we assess the efficiency and accuracy of the proposed method, on the basis of numerical results obtained for benchmark problems having available analytical solution.

Keywords: `Elastodynamic wave propagation, soft scattering, space-time boundary integral equation, energetic boundary element method`

AMS subject classification: `65M38`

1. Introduction

Linear elastodynamic two-dimensional problems are ideally suited to successful applications of boundary integral equation (BIE) approaches and to their discretizations into boundary elements methods (BEM) (see [1], [2]). An excellent review of the application of the BIE formulations and BEMs to elastic wave propagation problems can be found in [3]. Frequently claimed advantages over domain approaches are the dimensionality reduction, the easy implicit enforcement of radiation conditions at infinity and the achievable accuracy.

In principle, both the frequency-domain and time-domain BEM can be used for elastodynamic wave propagation problems. The first boundary integral formulation for elastodinamics was published by Cruse and Rizzo [4]. This formulation operates in Laplace domain with a subsequent inverse transformation to the time domain to achieve results for the transient behavior. The corresponding formulation in Fourier domain, i.e. frequency domain, was presented by Dominguez [5]. For recent development of frequency-domain methods, see e.g. [6], [7]. However, since all numerical inversion formulas from frequency-domain to time-domain depend on a proper choice of parameters, a direct evaluation in time-domain seems to be preferable. Moreover, it is more natural to work in the real time-domain and observe the phenomenon as it evolves.

Time-domain BIE formulations were developed more recently primarily by soil-structure interaction problems (see e.g. [8], [9], [10], [11]). Time-domain approaches can be further classified into time-stepping methods and the space-time integral equation methods. The former are based on a time discretization of the original initial-boundary value problem via an implicit scheme and on the use of BIEs to solve the resulting elliptic problems for each time step; the latter start from the space-time fundamental solutions of the differential operator at hand in order to construct BIEs via representation formulas and jump relations.

The mathematical analysis of elastodynamic BIE techniques in both space and time is based on a variational method [12] which furnishes genuine convergence results, following the pioneering papers [13], [14]

on space-time Galerkin BEMs for scalar wave propagation. The way to obtain this weak formulation and to prove stability results may be summarized in the following steps: Laplace or Fourier transform in time variable; uniform estimates with respect to complex frequencies of the corresponding Helmoltz problem; application of the Paley-Wienner theorem and Parseval identity. The drawback of this method is that the passage to complex frequencies leads to stability constants that grow exponentially in time ([15], [16]). Further, in this approach a challenge is represented by an adequate choice of the time-step size, in order to avoid numerical instabilities. Another technique to be mentioned is the convolution quadrature method for time discretizaton, developed in [17], [18], [19]. It provides a straightforward way to obtain a stable time stepping scheme using the Laplace transform of the kernel functions.
In this paper we consider a Dirichlet problem for a temporally homogeneous two-dimensional elastodynamic equation, reformulated as an indirect BIE; in particular we aim at extending to 2D elastodynamic soft scattering problems a recently developed space-time weak formulation of the BIEs related to scalar wave propagation phenomena. This weak formulation is called *energetic*, because it takes advantage of some properties of the energy of the system ([20], [21]). The Energetic BEM has been applied so far to many models: interior and exterior 2D ([21], [22], [23]) and 3D ([24], [25]) scalar wave propagation problems and, more recently, 2D exterior damped wave propagation problems ([26], [27]). Obtained numerical results are very interesting in comparison with other ones found in literature ([28]).
The paper is organized as follows: in Section 2 and 3 the model problem and its energetic BIE weak formulation are presented, respectively. Section 4 is devoted to subsequent energetic Galerkin BEM discretization. In Section 5 several numerical results are presented and discussed, in relation to benchmarks having available analytical solution. Conclusions are summarized in the last Section.

2. Model problem

We analyze the Navier problem in a bounded time interval $[0,T]$ outside an open arc $\Gamma \subset \mathbb{R}^2$, equipped by Dirichlet boundary conditions and homogeneous initial conditions. In acoustics, the exterior Dirichlet problem defines the scattering of a plane wave at a soft obstacle [29], hence the model problem here taken into account will be analogously referred to as elastodynamic soft scattering.
A coordinate system $(\mathbf{x},t)$ is employed, where $\mathbf{x} = (x_1,x_2)^\top$ denotes the cartesian spatial coordinates and t is the time. If Γ^- and Γ^+ denote the lower and upper faces of the arc Γ, respectively, $\mathbf{n} = (n_1,n_2)^\top$ defines the normal unit vector to Γ oriented from Γ^- to Γ^+. The differential problem, in the unknown displacement field $\mathbf{u} = (u_1,u_2)^\top$, reads:

$$(\lambda+\mu)\nabla(\nabla\cdot\mathbf{u}) + \mu\Delta\mathbf{u} + \rho\mathbf{b} = \rho\ddot{\mathbf{u}} \qquad \mathbf{x}\in\mathbb{R}^2\backslash\Gamma\,,\ t\in(0,T] \tag{1}$$

$$\mathbf{u}(\mathbf{x},0) = \dot{\mathbf{u}}(\mathbf{x},0) = 0 \qquad \mathbf{x}\in\mathbb{R}^2\backslash\Gamma \tag{2}$$

$$\mathbf{u}(\mathbf{x},t) = \bar{\mathbf{u}}(\mathbf{x},t) \qquad (\mathbf{x},t)\in\Sigma := \Gamma\times(0,T] \tag{3}$$

where $\lambda,\mu>0$ are the so-called Lamé parameters, $\rho>0$ is the mass density, $\mathbf{b}(\mathbf{x},t)$ is a given body-force vector and $\bar{\mathbf{u}}(\mathbf{x},t)$ is the Dirichlet datum. Furthermore, upper dots indicate time differentiation.
Writing (1)-(3) by components, for $i=1,2$ one has:

$$\sum_{h,k,l=1}^{2}\frac{\partial}{\partial x_k}\left(C_{ih}^{kl}\frac{\partial}{\partial x_h}\right)u_l(\mathbf{x},t) + \rho b_i(\mathbf{x},t) = \rho\ddot{u}_i(\mathbf{x},t) \qquad \mathbf{x}\in\mathbb{R}^2\backslash\Gamma, t\in[0,T] \tag{4}$$

$$u_i(\mathbf{x},0) = \dot{u}_i(\mathbf{x},0) = 0 \qquad \mathbf{x}\in\mathbb{R}^2\backslash\Gamma \tag{5}$$

$$u_i(\mathbf{x},t) = \bar{u}_i(\mathbf{x},t) \qquad (\mathbf{x},t)\in\Sigma\,. \tag{6}$$

In (4), C_{ih}^{kl} is the Hooke tensor, that depends only on the two independent Lamé elastic constants λ,μ and on the Kronecker delta:

$$C_{ih}^{kl} = \lambda\delta_{ih}\delta_{kl} + \mu(\delta_{ik}\delta_{hl} + \delta_{il}\delta_{hk}) \qquad i,h,k,l = 1,2 \tag{7}$$

and whose symmetry properties are summarized by

$$C_{ih}^{kl} = C_{hi}^{kl} = C_{ih}^{lk} = C_{kl}^{ih} \,. \tag{8}$$

The traction vector is defined through this tensor as

$$p_i(\mathbf{x},t) := \sum_{h,k,l=1}^{2} C_{ih}^{kl}\, \frac{\partial u_k}{\partial x_l}(\mathbf{x},t) n_h \qquad i=1,2\,. \tag{9}$$

The displacement $\mathbf{u}$ may be decomposed into an irrotational (or dilatational) part $\mathbf{u}_{\mathrm{P}}$ and a rotational (or equivoluminal) part $\mathbf{u}_{\mathrm{S}}$, i.e.

$$\mathbf{u} = \mathbf{u}_{\mathrm{P}} + \mathbf{u}_{\mathrm{S}}\,,$$

naming $\mathbf{u}_{\mathrm{P}}$ primary (or pressure or compressional) and $\mathbf{u}_{\mathrm{S}}$ secondary (or shear or solenoidal) waves; the propagation velocities of the pressure and shear waves in the medium are given, respectively, as

$$c_{\mathrm{P}}^2 = (\lambda+2\mu)/\rho\,, \qquad c_{\mathrm{S}}^2 = \mu/\rho \tag{10}$$

and therefore $c_{\mathrm{P}} > c_{\mathrm{S}}$.

3. Fundamental solution and energetic BIE weak formulation

In order to approximate $\mathbf{u}(\mathbf{x},t)$ using a BEM technique, we have to obtain a boundary integral reformulation of the problem (4) – (6). This can be done using classical arguments and the knowledge of the fundamental solution of the two-dimensional differential operator at hand. The full-space Green's function is a second order tensor with components $G_{ij}(\mathbf{x},\boldsymbol{\xi};t,\tau)$, $i,j=1,2$, that satisfies the Green's identity in relation to Navier operator in (4). Hence it is fundamental solution of the equations

$$\sum_{h,k,l=1}^{2} \frac{\partial}{\partial x_h}\Big(C_{ih}^{kl}\frac{\partial}{\partial x_l}\Big) G_{kj}(\mathbf{x},\boldsymbol{\xi};t,\tau) + \rho b_{ij}(\mathbf{x},t) = \rho\, \ddot{G}_{ij}(\mathbf{x},\boldsymbol{\xi};t,\tau) \tag{11}$$

$$\mathbf{x},\boldsymbol{\xi} \in \mathbb{R}^2,\ \ \tau < t\,, \qquad i,j=1,2\,,$$

when applying the space-time point body-force

$$\rho\, b_{ij}(\mathbf{x},t) = \delta_{ij}\, \delta(\mathbf{x}-\boldsymbol{\xi})\delta(t-\tau)\ .$$

Since coefficients in (1) are independent of space and time, the Green's function depends on the arguments $\mathbf{x},\boldsymbol{\xi},t,\tau$ only through the differences $t-\tau$, $r_i = x_i - \xi_i$, $i=1,2$ and $r = \|\mathbf{x}-\boldsymbol{\xi}\|_2$:

$$\begin{aligned} &G_{ij}(\mathbf{x},\boldsymbol{\xi};t,\tau) = \\ &\frac{1}{2\pi\rho}\Bigg\{ \frac{H[c_{\mathrm{P}}(t-\tau)-r]}{c_{\mathrm{P}}} \left[\frac{2c_{\mathrm{P}}^2(t-\tau)^2 - r^2}{\sqrt{c_{\mathrm{P}}^2(t-\tau)^2 - r^2}} \cdot \frac{r_i r_j}{r^4} - \frac{\delta_{ij}}{r^2} \cdot \sqrt{c_{\mathrm{P}}^2(t-\tau)^2 - r^2} \right] \\ &- \frac{H[c_{\mathrm{S}}(t-\tau)-r]}{c_{\mathrm{S}}} \left[\frac{2c_{\mathrm{S}}^2(t-\tau)^2 - r^2}{\sqrt{c_{\mathrm{S}}^2(t-\tau)^2 - r^2}} \cdot \frac{r_i r_j}{r^4} - \frac{\delta_{ij}}{r^2} \cdot \frac{c_{\mathrm{S}}^2(t-\tau)^2}{\sqrt{c_{\mathrm{S}}^2(t-\tau)^2 - r^2}} \right] \Bigg\}, \\ &\qquad\qquad\qquad\qquad\qquad\qquad\qquad\qquad\qquad\qquad\qquad\qquad i,j=1,2 \end{aligned} \tag{12}$$

and it satisfies the space-time reciprocity relation

$$G_{ij}(\mathbf{x},\boldsymbol{\xi};t,\tau) = G_{ji}(\boldsymbol{\xi},\mathbf{x};t,\tau)\,. \tag{13}$$

For the application of BEM, the starting point is an integral representation formula over Σ for the solution of the differential problem (1) – (3).

In case of sole Dirichlet boundary conditions an indirect formulation, deduced from Somigliana reciprocity identity, can be used:

for $(\mathbf{x},t)\in(\mathbb{R}^2\backslash\Gamma)\times(0,T]$ *and* $i=1,2$

$$u_i(\mathbf{x},t)=\sum_{j=1}^{2}\int_0^t\int_\Gamma G_{ij}(\mathbf{x},\boldsymbol{\xi};t,\tau)\phi_j(\boldsymbol{\xi},\tau)\,\mathrm{d}\Gamma_{\boldsymbol{\xi}}\mathrm{d}\tau+ \sum_{j=1}^{2}\int_0^t\int_{\mathbb{R}^2\backslash\Gamma} G_{ij}(\mathbf{x},\boldsymbol{\xi};t,\tau)\rho b_j(\boldsymbol{\xi},\tau)\,\mathrm{d}\Omega_{\boldsymbol{\xi}}\mathrm{d}\tau \tag{14}$$

where $\boldsymbol{\phi}=(\phi_1,\phi_2)^\top$ is an unknown vector defined over Σ and belonging to the same functional space of $\mathbf{p}=(p_1,p_2)^\top$.
In the following, null body-forces will be assumed, hence leading, with a limiting process for $\mathbf{x}$ tending to the boundary, to the BIEs

$$u_i(\mathbf{x},t)=\sum_{j=1}^{2}\int_0^t\int_\Gamma G_{ij}(\mathbf{x},\boldsymbol{\xi};t,\tau)\phi_j(\boldsymbol{\xi},\tau)\,\mathrm{d}\Gamma_{\boldsymbol{\xi}}\mathrm{d}\tau \qquad (\mathbf{x},t)\in\Sigma\,,\quad i=1,2\,. \tag{15}$$

Now, introducing the space-time integral operators

$$\begin{aligned}&\mathcal{V}_{ij}: L^2([0,T];H^{-\frac{1}{2}}(\Gamma))\to H^1([0,T];H^{\frac{1}{2}}(\Gamma))\\ &[\mathcal{V}_{ij}\phi_j](\mathbf{x},t):=\int_0^t\int_\Gamma G_{ij}(\mathbf{x},\boldsymbol{\xi};t,\tau)\phi_j(\boldsymbol{\xi},\tau)\,\mathrm{d}\Gamma_{\boldsymbol{\xi}}\mathrm{d}\tau\,,\qquad i,j=1,2\end{aligned} \tag{16}$$

the BIEs (15), can be written in the compact form

$$\sum_{j=1}^{2}[\mathcal{V}_{ij}\phi_j](\mathbf{x},t)=u_i(\mathbf{x},t),\quad i=1,2 \tag{17}$$

and using the boundary condition (3), we can write down a system of two BIEs in the boundary unknown $\boldsymbol{\phi}$:

$$\begin{pmatrix}\mathcal{V}_{11}&\mathcal{V}_{12}\\ \mathcal{V}_{21}&\mathcal{V}_{22}\end{pmatrix}\begin{pmatrix}\phi_1(\mathbf{x},t)\\ \phi_2(\mathbf{x},t)\end{pmatrix}=\begin{pmatrix}\overline{u}_1(\mathbf{x},t)\\ \overline{u}_2(\mathbf{x},t)\end{pmatrix}. \tag{18}$$

At this stage, we remark that the solution of (1) – (3) with null body-forces satisfies the following energy identity

$$\begin{aligned}\mathcal{E}(\mathbf{u},T):=&\frac{1}{2}\sum_{i=1}^{2}\int_{\mathbb{R}^2\backslash\Gamma}\Big[\rho\,\dot{u}_i^2(\mathbf{x},T)+\sum_{h=1}^{2}\sum_{k,l=1}^{2}C_{ih}^{kl}\frac{\partial u_i}{\partial x_h}(\mathbf{x},T)\frac{\partial u_k}{\partial x_l}(\mathbf{x},T)\Big]\mathrm{d}\mathbf{x}\\ =&\sum_{i=1}^{2}\int_\Gamma\int_0^T\dot{u}_i(\mathbf{x},t)\phi_i(\mathbf{x},t)\mathrm{d}t\,\mathrm{d}\Gamma_{\mathbf{x}},\end{aligned} \tag{19}$$

which can be obtained by multiplying (4) by $\dot{u}_i(\mathbf{x},t)$, using the symmetry properties in (8), integrating over $(\mathbb{R}^2\backslash\Gamma)\times[0,T]$, then by parts in space variables and summing over index i. Hence, taking into account the components in (17), the energetic weak formulation of the system (18) is defined as follows:

find $\phi_i\in L^2([0,T];H^{-\frac{1}{2}}(\Gamma))$, *such that*

$$\sum_{j=1}^{2}<\dot{[\mathcal{V}_{ij}\phi_j]},\psi_i>_{L^2(\Sigma)}=<\dot{\overline{u}}_i,\psi_i>_{L^2(\Sigma)}\,,\qquad i=1,2 \tag{20}$$

where $\psi_i(\mathbf{x},t)$ are suitable test functions, belonging to the same functional space of $\phi_i(\mathbf{x},t)$, (see also [21], where the energetic weak formulation was introduced for scalar Dirichlet wave propagation problems). In particular equations in (18) are differentiated with respect to time and projected by means of $L^2(\Sigma)$ scalar product. Note that the involved scalar products are represented by a space-time integral hence we have to deal with a double integration in time variables and a double integration in space variables.

Remark. The energy $\mathcal{E}(\mathbf{u},T)$ can be also written in the compact form:

$$\mathcal{E}(\mathbf{u},T)=\frac{1}{2}\int_{\mathbb{R}^2\setminus\Gamma}\left[\rho\|\dot{\mathbf{u}}\|_2^2+\mu\|\nabla\mathbf{u}\|_F^2+(\lambda+\mu)(\nabla\cdot\mathbf{u})^2\right](\mathbf{x},t)d\mathbf{x} \tag{21}$$

where $\|\cdot\|_F$ indicates the Frobenius norm, which explicitly shows its positivity.

4. Galerkin BEM discretization

For time discretization we consider a uniform decomposition of the time interval $[0,T]$ with time step $\Delta t=T/N_{\Delta t}$, $N_{\Delta t}\in\mathbb{N}^+$, generated by the $N_{\Delta t}+1$ time-knots: $t_n=n\Delta t,\ n=0,\cdots,N_{\Delta t}$, and we choose piecewise constant shape functions for the temporal approximation of $\phi_i(\mathbf{x},t)$

$$v_n(t):=H[t-t_n]-H[t-t_{n+1}]\,. \tag{22}$$

For the space discretization we consider a boundary mesh $\mathcal{T}=\{e_1,\ldots,e_M\}$ on Γ constituted by M segments such that $\text{length}(e_i)\le\Delta x$, $e_i\cap e_j=\emptyset$ if $i\neq j$ and $\cup_{i=1}^M\bar{e}_i=\bar{\Gamma}$ (if the obstacle is not piece-wise linear the union of $\bar{e}_i$ will give a suitable approximation of $\bar{\Gamma}$). Having defined $\mathcal{P}_d$ the space of algebraic polynomials of degree d on the element $e_i\in\mathcal{T}$, we consider the space of piecewise polynomial functions

$$X_{-1,\Delta x}:=\{\,w\ \in\ L^2(\Gamma)\ |\ w_{|e_i}\in\mathcal{P}_d\,,\,\forall\,e_i\in\mathcal{T}\,\}\,. \tag{23}$$

Hence, denoted by $M_{\Delta x}$ the number of degrees of freedom on Γ and introduced the standard piecewise polynomial boundary element basis functions $w_m(\mathbf{x})$, $m=1,\cdots,M_{\Delta x}$, in $X_{-1,\Delta x}$, the components of the approximate solution of (20) will be expressed as

$$\phi_i(\mathbf{x},t)\cong\tilde{\phi}_i(\mathbf{x},t):=\sum_{n=0}^{N_{\Delta t}-1}\sum_{m=1}^{M_{\Delta x}}\alpha_{nm}^i w_m(\mathbf{x})v_n(t)\,. \tag{24}$$

and the test functions will be replaced by

$$\psi_i(\mathbf{x},t)=w_{\widetilde{m}}(\mathbf{x})v_{\widetilde{n}}(t)\,,\qquad\widetilde{m}=1,\cdots,M_{\Delta x}\,,\quad\widetilde{n}=0,\cdots,N_{\Delta t}-1\,.$$

The Galerkin BEM discretization coming from energetic weak formulation (20) produces the linear system

$$\mathbb{E}\boldsymbol{\alpha}=\boldsymbol{\beta}, \tag{25}$$

where matrix $\mathbb{E}$ has a block lower triangular Toeplitz structure, since its elements depend on the difference $t_{\tilde{n}}-t_n$ and in particular they vanish if $t_{\tilde{n}}\le t_n$. Each block has dimension $2M_{\Delta x}$. If we denote by $\mathbb{E}^{(\ell)}$ the block obtained when $t_{\tilde{n}}-t_n=(\ell+1)\Delta t$, $\ell=0,\ldots,N_{\Delta t}-1$, the linear system can be written as

$$\begin{pmatrix}\mathbb{E}^{(0)} & 0 & 0 & \ldots & 0\\ \mathbb{E}^{(1)} & \mathbb{E}^{(0)} & 0 & \ldots & 0\\ \mathbb{E}^{(2)} & \mathbb{E}^{(1)} & \mathbb{E}^{(0)} & \ldots & 0\\ \vdots & \vdots & \vdots & \ddots & \vdots\\ \mathbb{E}^{(N_{\Delta t}-1)} & \mathbb{E}^{(N_{\Delta t}-2)} & \mathbb{E}^{(N_{\Delta t}-3)} & \ldots & \mathbb{E}^{(0)}\end{pmatrix}\cdot\begin{pmatrix}\boldsymbol{\alpha}^{(0)}\\ \boldsymbol{\alpha}^{(1)}\\ \boldsymbol{\alpha}^{(2)}\\ \vdots\\ \boldsymbol{\alpha}^{(N_{\Delta t}-1)}\end{pmatrix}=\begin{pmatrix}\boldsymbol{\beta}^{(0)}\\ \boldsymbol{\beta}^{(1)}\\ \boldsymbol{\beta}^{(2)}\\ \vdots\\ \boldsymbol{\beta}^{(N_{\Delta t}-1)}\end{pmatrix} \tag{26}$$

where the unknowns and rhs entries are organized as follows

$$\begin{aligned}\boldsymbol{\alpha}^{(\ell)} &= \left(\alpha^1_{\ell 1},\cdots,\alpha^1_{\ell M_{\Delta x}},\alpha^2_{\ell 1},\cdots,\alpha^2_{\ell M_{\Delta x}}\right)^\top,\\ \boldsymbol{\beta}^{(\ell)} &= \left(\beta^1_{\ell 1},\cdots,\beta^1_{\ell M_{\Delta x}},\beta^2_{\ell 1},\cdots,\beta^2_{\ell M_{\Delta x}}\right)^\top.\end{aligned} \tag{27}$$

The solution of (26) is obtained by a block forward substitution, i.e. at every time instant $t_\ell = (\ell+1)\Delta t$, $\ell = 0,\cdots,N_{\Delta t}-1$, one computes

$$\mathbf{z}^{(\ell)} = \boldsymbol{\beta}^{(\ell)} - \sum_{j=1}^{\ell} \mathbb{E}^{(j)}\boldsymbol{\alpha}^{(\ell-j)} \tag{28}$$

and then solves the reduced linear system

$$\mathbb{E}^{(0)}\boldsymbol{\alpha}^{(\ell)} = \mathbf{z}^{(\ell)}\,. \tag{29}$$

Procedure (28) – (29) is a time-marching technique, where the only matrix to be inverted is the non-singular block $\mathbb{E}^{(0)}$; therefore the LU factorization needs to be performed only once and stored. Then, at each time step, the solution of (29) requires only a forward and a backward substitution phases. All the other blocks $\mathbb{E}^{(\ell)}$ are used to update at every time step the right-hand side. Of course, due to the whole matrix $\mathbb{E}$ structure, one can construct and store only blocks $\mathbb{E}^{(0)},\cdots,\mathbb{E}^{(N_{\Delta t}-1)}$ with a considerable reduction in computational cost and memory requirement.

The matrix entries in the $\mathbb{E}^{(\ell)}$-block are

$$\begin{aligned}&< [\mathcal{V}_{ij}\,\dot{w}_m\,v_n], w_{\tilde m}\,v_{\tilde n} >_{L^2(\Sigma)} =\\ &\int_0^T\int_\Gamma w_{\tilde m}(\mathbf{x})\,v_{\tilde n}(t)\frac{\partial}{\partial t}\Big(\int_0^t\int_\Gamma G_{ij}(\mathbf{x},\boldsymbol{\xi};t,\tau)\,w_m(\boldsymbol{\xi})\,v_n(\tau)\mathrm{d}\Gamma_{\boldsymbol{\xi}}\mathrm{d}\tau\Big)\mathrm{d}\Gamma_{\mathbf{x}}\mathrm{d}t,\\ &\qquad i,j=1,2\,;\quad \tilde n,n=0,\cdots,N_{\Delta t}-1\,;\quad \tilde m,m=1,\cdots,M_{\Delta x}\,.\end{aligned} \tag{30}$$

Remembering that $r_i := x_i-\xi_i$, $i=1,2$ and defining $\Delta_{\tilde n+h,n+k} := t_{\tilde n+h}-t_{n+k}$, after a double analytic integration in the time variables, we have

$$\begin{aligned}&< [\mathcal{V}_{ij}\,\dot{w}_m\,v_n], w_{\tilde m}\,v_{\tilde n} >_{L^2(\Sigma)} =\\ &\quad -\sum_{h,k=0}^{1}\frac{(-1)^{h+k}}{2\pi\rho}\int_\Gamma w_{\tilde m}(\mathbf{x})\int_\Gamma w_m(\boldsymbol{\xi})V_{ij}(r;\Delta_{\tilde n+h,n+k})\mathrm{d}\Gamma_{\boldsymbol{\xi}}\,\mathrm{d}\Gamma_{\mathbf{x}}\end{aligned} \tag{31}$$

where

$$\begin{aligned}&V_{ij}(r;\Delta_{\tilde n+h,n+k}) := \Big(\frac{r_ir_j}{r^4}-\frac{\delta_{ij}}{2r^2}\Big)\\ &\Big[\frac{H[c_{\mathrm{P}}\Delta_{\tilde n+h,n+k}-r]}{c_{\mathrm{P}}^2}\varphi_{\mathrm{P}}(r;\Delta_{\tilde n+h,n+k})-\frac{H[c_{\mathrm{S}}\Delta_{\tilde n+h,n+k}-r]}{c_{\mathrm{S}}^2}\varphi_{\mathrm{S}}(r;\Delta_{\tilde n+h,n+k})\Big]+\\ &\frac{\delta_{ij}}{2}\Big[\frac{H[c_{\mathrm{P}}\Delta_{\tilde n+h,n+k}-r]}{c_{\mathrm{P}}^2}\tilde\varphi_{\mathrm{P}}(r;\Delta_{\tilde n+h,n+k})+\frac{H[c_{\mathrm{S}}\Delta_{\tilde n+h,n+k}-r]}{c_{\mathrm{S}}^2}\tilde\varphi_{\mathrm{S}}(r;\Delta_{\tilde n+h,n+k})\Big]\end{aligned} \tag{32}$$

having set

$$\begin{aligned}&\varphi_\gamma(r;\Delta_{\tilde n+h,n+k}) := c_\gamma\Delta_{\tilde n+h,n+k}\sqrt{c_\gamma^2\Delta^2_{\tilde n+h,n+k}-r^2}\,,\\ &\tilde\varphi_\gamma(r;\Delta_{\tilde n+h,n+k}) := \log\left(c_\gamma\Delta_{\tilde n+h,n+k}+\sqrt{c_\gamma^2\Delta^2_{\tilde n+h,n+k}-r^2}\right)-\log r\end{aligned} \tag{33}$$

in which $\gamma = \mathrm{P}, \mathrm{S}$. In (32), the Heaviside functions represent the wave front propagation and their contribution is 0 or 1.
If $r < c_{\mathrm{S}}\Delta_{\tilde{n}+h,n+k} < c_{\mathrm{P}}\Delta_{\tilde{n}+h,n+k}$, then (32) reduces to

$$
\begin{aligned}
&V_{ij}(r;\Delta_{\tilde{n}+h,n+k}) := \\
&\frac{c_{\mathrm{P}}^2 - c_{\mathrm{S}}^2}{c_{\mathrm{P}}c_{\mathrm{S}}}\Big(\frac{r_i r_j}{r^2} - \frac{\delta_{ij}}{2}\Big)\frac{\Delta_{\tilde{n}+h,n+k}}{c_{\mathrm{P}}\sqrt{c_{\mathrm{S}}^2\Delta_{\tilde{n}+h,n+k}^2 - r^2} + c_{\mathrm{S}}\sqrt{c_{\mathrm{P}}^2\Delta_{\tilde{n}+h,n+k}^2 - r^2}} - \\
&\frac{c_{\mathrm{P}}^2 + c_{\mathrm{S}}^2}{c_{\mathrm{P}}^2 c_{\mathrm{S}}^2}\frac{\delta_{ij}}{2}\log r + \frac{\delta_{ij}}{2}\Big[\frac{1}{c_{\mathrm{P}}^2}\log\Big(c_{\mathrm{P}}\Delta_{\tilde{n}+h,n+k} + \sqrt{c_{\mathrm{P}}^2\Delta_{\tilde{n}+h,n+k}^2 - r^2}\Big) + \\
&\frac{1}{c_{\mathrm{S}}^2}\log\Big(c_{\mathrm{S}}\Delta_{\tilde{n}+h,n+k} + \sqrt{c_{\mathrm{S}}^2\Delta_{\tilde{n}+h,n+k}^2 - r^2}\Big)\Big]
\end{aligned}
\tag{34}
$$

and we observe a space singularity of type $\mathcal{O}(\log r)$ as $r \to 0$, which is typical of weakly singular kernels related to $2D$ elliptic problems. The adopted quadrature strategy is a (not trivial) extension of the procedure used in [21] for Energetic BEM applied to scalar wave propagation problems.

For what concerns the overall computational cost of the Energetic BEM, it is due to three phases: (i) construction of $\mathbb{E}^{(\ell)}$ blocks; (ii) numerical solution of linear systems (29); (iii) post-processing evaluation of displacements by representation formula (14), once the unknown $\boldsymbol{\phi}$ is recovered.
The first step is the heaviest, since it involves the evaluation of double boundary integrals (31) with the suitable quadrature schemes just cited. Anyway, since matrices $\mathbb{E}^{(\ell)}$ are independent of each other, this phase can be speeded up using concurrent processors doing blocks evaluation in parallel. The second step can be fastened using a FFT-based algorithm as described and analyzed in [27]. The last phase has computational cost directly proportional to the number of space-time points $(\mathbf{x}, t) \in \mathbb{R}^2\backslash\Gamma \times (0, T]$ where one needs to evaluate displacements field. In particular, for the considered model problem, having set $\Delta_{t,n+k} := t - t_{n+k}$, one has to compute the following expressions, for $i = 1, 2$:

$$
u_i(\mathbf{x}, t) = \sum_{j=1}^{2}\sum_{n=0}^{N_{\Delta t}-1}\sum_{m=1}^{M_{\Delta x}}\sum_{k=0}^{1}\frac{(-1)^k}{2\pi\rho}\,\alpha_{nm}^{j}\int_{\Gamma} V_{ij}(r;\Delta_{t,n+k})\,w_m(\boldsymbol{\xi})\,\mathrm{d}\Gamma_{\boldsymbol{\xi}}
\tag{35}
$$

using standard Gauss-Legendre quadrature rule for the evaluation of the non-singular boundary integrals.

Remark. The marching-on-time scheme is implicit and unconditionally stable, as proved for scalar problems in [30], [31], [32] in the more general framework of Energetic BEM-FEM coupling.

5. Numerical results

In this Section we present several numerical results related to benchmark problems with available reference analytical solution.
At first, we fix $c_{\mathrm{S}} = c_{\mathrm{P}}$, i.e. we consider an academic test having no physical meaning (see (10)) with the aim of reducing the elastodynamic BIE system (18) to two uncoupled scalar BIEs related to the vector wave propagation problem

$$
\mu\Delta\mathbf{u} - \rho\ddot{\mathbf{u}} = 0
\tag{36}
$$

in order to check the vectorial extension of Energetic BEM w.r.t. its scalar version. In fact, kernels (12) assume the following expression

$$
G_{ij}(\mathbf{x}, \boldsymbol{\xi}; t, \tau) = \frac{\delta_{ij}}{2\pi\rho\, c_{\mathrm{S}}}\,\frac{H[c_{\mathrm{S}}(t-\tau) - r]}{\sqrt{c_{\mathrm{S}}^2(t-\tau)^2 - r^2}}\,, \qquad i, j = 1, 2
\tag{37}
$$

which, for $i = j$, represents the two-dimensional fundamental solution of the scalar wave operator. In this framework, we consider a straight obstacle

$$\Gamma = \{(x_1, 0) \,|\, x_1 \in [-0.5, 0.5]\} \tag{38}$$

and we fix $c_{\mathrm{S}} = c_{\mathrm{P}} = 1$ and $\rho = 1$. The assigned Dirichlet boundary condition is

$$\bar{u}_i(x_1, t) = H[t]\, f(t)\, x_1\,, \quad i = 1, 2 \tag{39}$$

where

$$f(t) := \begin{cases} \sin^2(4\pi\, t) & \text{if } t \in [0, 1/8] \\ 1 & \text{if } t \geq 1/8 \end{cases}.$$

Since the Dirichlet datum becomes independent of time, for $t \geq 1/8$, we expect that each component $\phi_i(x_1, t)$ of the approximate transient BIEs system solution will tend to the BIE solution ϕ_∞ related to the stationary Laplace problem defined in $\mathbb{R}^2 \setminus \Gamma$ and equipped by Dirichlet datum $\bar{u}(x_1) = x_1$. This reference static solution is analytically known and it reads

$$\phi_\infty(x_1) = \frac{2\, x_1}{\sqrt{1/4 - x_1^2}}\,.$$

In Figure 1 we show the time history of both the components of the energetic BIEs solution at the point of Γ with $x_1 = 0.25$ and on the time interval $[0, 2]$, for different values of the discretization parameters, having chosen piece-wise constant space-time basis functions. Let us note that when we refine Δx and Δt, the energetic solution is better described in the initial temporal phase, but both the simulations tend to the same constant value which approximates $\phi_\infty(0.25)$. The peak is due to the growing phase of the Dirichlet datum, then the considered boundary point is solicited again at $t = 0.25$ by the wave generated at the right endpoint of Γ travelling with unitary velocity.

In Figure 2, the reader can observe results related to doubled velocities and obtained by Energetic BEM

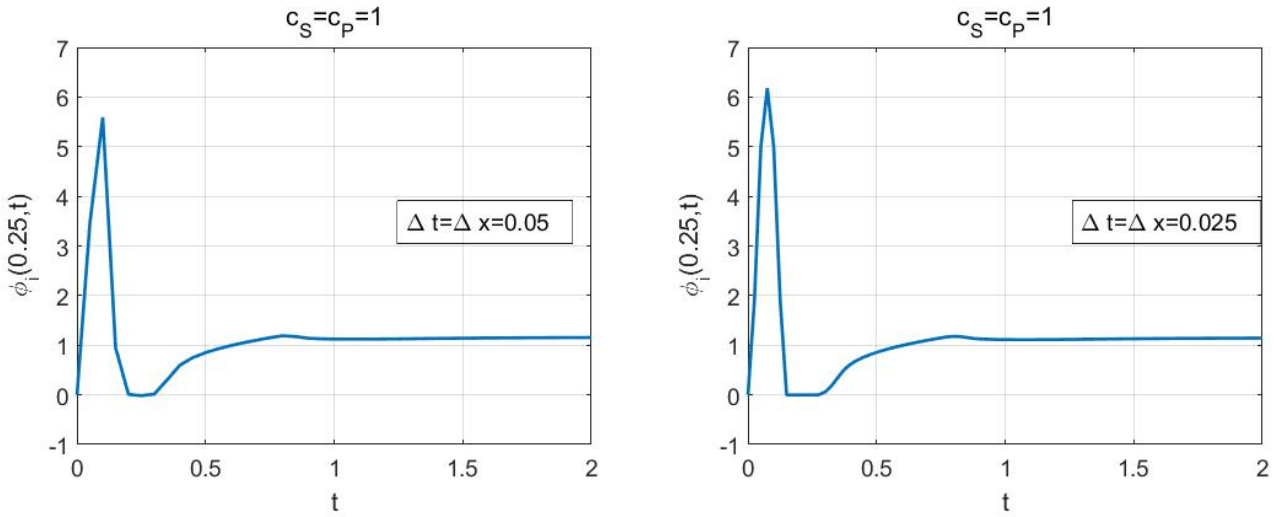

Figure 1. $\phi_i(0.25, t)$, $i = 1, 2$ evaluated by Energetic BEM using different discretization parameters, for $c_{\mathrm{S}} = c_{\mathrm{P}} = 1$.

fixing $\Delta x = 0.05$ and $\Delta t = 0.025$. The peak time and height are halved and the solicitation from the right endpoint comes at $t = 0.125$.

Now, let us consider the same straight obstacle, but different primary and secondary velocities. In this case, the elastodynamic BIEs system can be still decoupled, because in the G_{ij} kernels (12) we can set

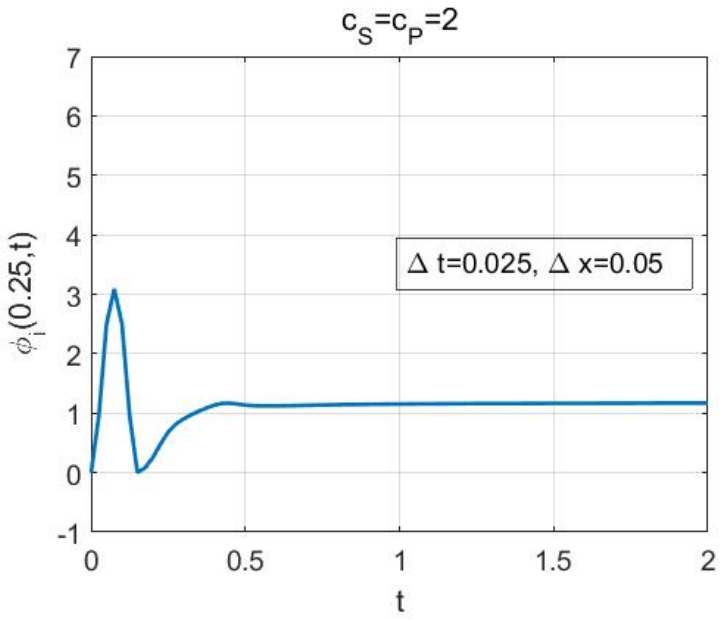

Figure 2. $\phi_i(0.25, t)$, $i = 1, 2$ evaluated by Energetic BEM, for $c_S = c_P = 2$.

$r_2 = 0$. Further, if we assign the Dirichlet datum (39), we expect a transient solution converging to the solution $\boldsymbol{\phi}_\infty$ of the elastostatic BIE with Dirichlet datum $\bar{u}_i(x_1) = x_1$, $i = 1, 2$, which is analytically known and reads

$$\phi_{i,\infty}(x_1) = \frac{2\, c_P^2}{c_S^2 + c_P^2} \frac{2\, x_1}{\sqrt{1/4 - x_1^2}}, \quad i = 1, 2\,.$$

In Figure 3, the vertical component $\phi_2(0.25, t)$ of the transient solution is shown on the time interval $[0, 2]$, for different values of the discretization parameters, having fixed $c_S = 1$ and $c_P = 2$ and piece-wise constant space-time basis functions. When we choose Δx and Δt in such a way that their ratio is equal to c_P we observe a better description of the initial evolution of the approximate solution than the choice $\Delta x/\Delta t = c_S$, but in any case the asymptotic behavior of the solution is perfectly kept by all Energetic BEM simulations. In Figure 4, we display the components $\phi_i(0.25, t)$, $i = 1, 2$ of the elastodynamic BIEs solution obtained for $\Delta x = 0.025$, $\Delta t = 0.0125$. While at the beginning of the simulation, the behavior of the graphs is different, both curves tend to the same limit value, given by $\phi_{i,\infty}(0.25)$.
At last, Figure 5 shows, on the time interval $[0, 10]$, the time history of the relative gap evaluated in $L^2(\Gamma)$ norm between the vertical components of analytical stationary and transient BIEs solutions, using for the latter Energetic BEM applied with different discretization parameters, in such a way that $\Delta x/\Delta t = c_P$. The smaller the parameters, the better the limit error.

For a quantitative evaluation of error reduction, we report in Table 1 the absolute value of the difference between transient approximate solution and limit stationary one evaluated in different points of Γ and for different time instants. Let us note that the uniform decomposition employed on Γ is not able to completely catch the weak singularity of the solution at the obstacle endpoints, and this is the reason for the behavior of the error, which anyway around the midpoint of Γ and for sufficiently high time decades linearly w.r.t. the discretization parameters. Non-uniform algebraically or geometrically graded meshes, defined in [33] and already used in [34] for Galerkin BEM applied to elliptic problems, are optimal for this kind of BIE solutions behavior and their inclusion into the Energetic BEM code is scheduled as next work.

Figures 6 and 7 show results obtained fixing $c_S = 1$, $c_P = 4$ and, as we can see, they are similar to those shown in Figures 3 and 4.

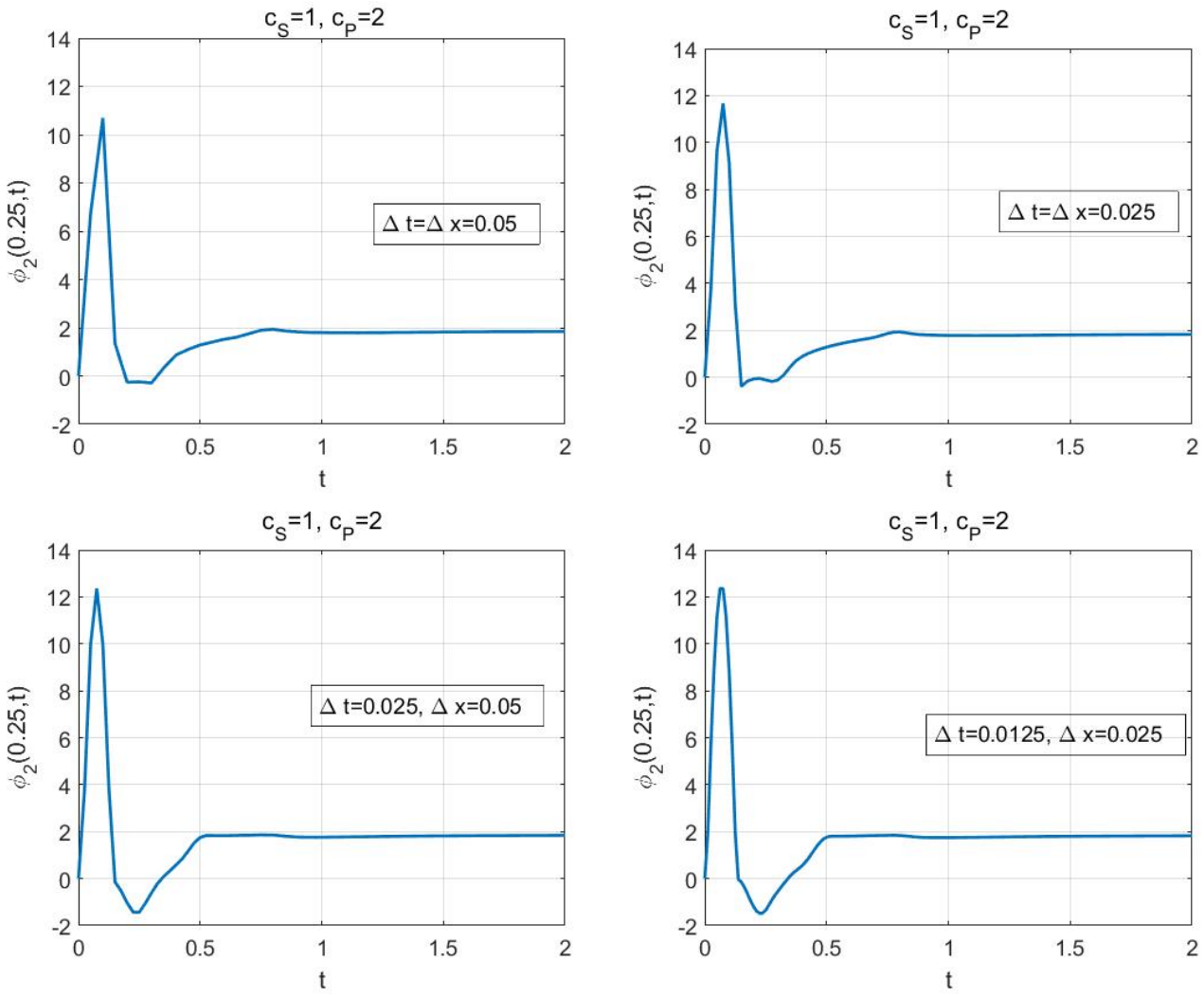

Figure 3. Vertical component $\phi_2(0.25, t)$ of the transient solution on the time interval $[0, 2]$, for different values of the discretization parameters, for $c_S = 1$, $c_P = 2$.

Finally, in Figure 8 we show $\phi_i(x_1, 2)$ compared to $\phi_{i,\infty}(x_1)$, for $i = 1, 2$: overlapping is already perfectly evident at $T = 2$, except at the endpoints of Γ where the analytical solution of the elastostatic problem presents a high gradient.

At last, on the same domain of the previous test problems and for $c_S = 1$, $c_P = 2$, we consider a Dirichlet datum given by $\bar{u}_1(\cdot, t) = 0$ and $\bar{u}_2(\cdot, t)$ shown in Figure 9, and we fix the observation time interval $[0, 10]$. As uniform time and space discretization steps we use $\Delta t = 0.05$ and $\Delta x = 0.1$ respectively and we adopt, as usual, piece-wise constant space-time shape and test functions.

In Figure 10 we show the time history of the density ϕ_2 obtained in the midpoint of Γ. As one can note, it has the same form of the derivative of the boundary datum and hence it vanishes for long times.

In Figure 11 the time history of the vertical displacement $u_2(\mathbf{x}, t)$ in $\mathbf{x} = (0, 3)$ (left) and $\mathbf{x} = (0, 5)$ (right) is plotted: the primary perturbation, traveling with $c_P = 2$, reaches the observation point at time instant $t = 0.5(x_2 + 1)$, while the tail traveling with $c_S = 1$ produces a much smaller perturbation at $t = x_2 + 0.5$. The greater the distance from Γ, the smaller both the solicitations. The horizontal displacement u_1 is negligible and it is not shown.

In Figure 12 we present a section of the vertical component $u_2(\mathbf{x}, t)$ of the solution of the original differential problem (1)-(3), along the segment $x_1 = 0$ and $0 < x_2 < 10$, at time instants $t = 2, 3, 4$:

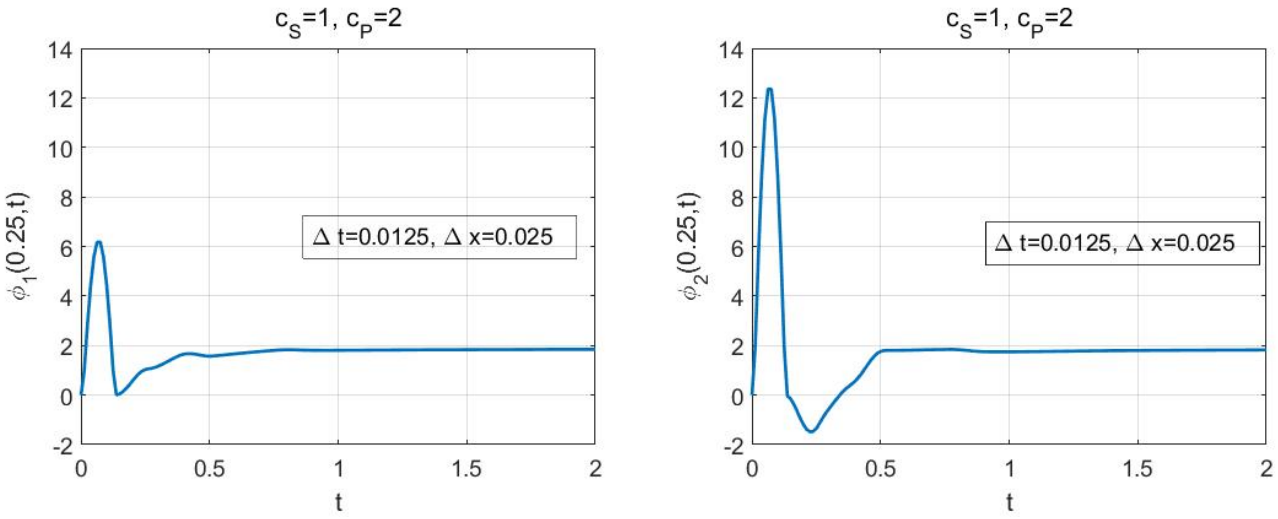

Figure 4. $\phi_i(0.25, t)$, $i = 1, 2$ evaluated by Energetic BEM, for $c_S = 1$, $c_P = 2$.

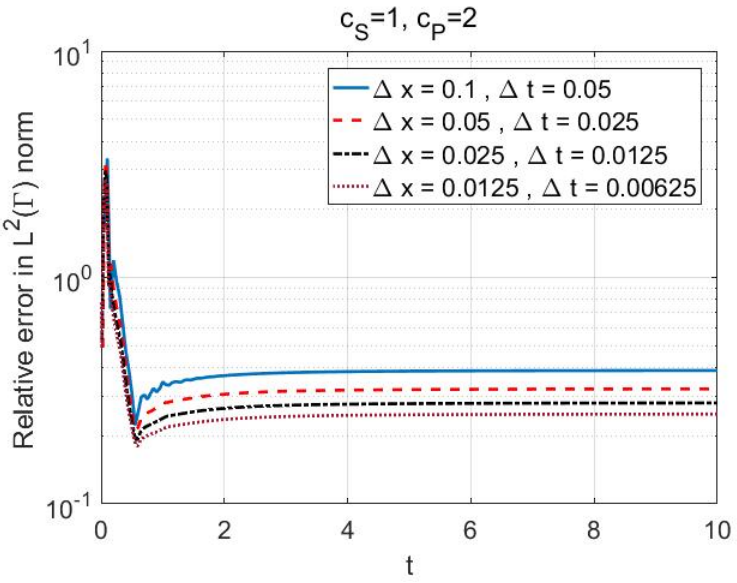

Figure 5. Time history of relative error in $L^2(\Gamma)$ norm, for different values of discretization parameters and for $c_S = 1$, $c_P = 2$.

as one can observe, both the perturbations, traveling away from the boundary Γ with different speeds $c_P = 2$, $c_S = 1$, assume the same structure of the Dirichlet boundary datum but with diminishing intensity for growing time. The higher the time, the greater the space distance between the two traveling waves.

6. Conclusions

In this paper, for the first time, Energetic BEM is applied to two-dimensional exterior elastodynamic problems, equipped by Dirichlet boundary condition. The extension of the method from 2D scalar wave propagation, even if not straightforward, has revealed to retain the optimal properties theoretically proved and numerically observed for the simpler model problem. Ongoing research is focused on the Energetic BEM treatment of elastodynamic space-time double layer potential and hypersingular boundary integral operator.

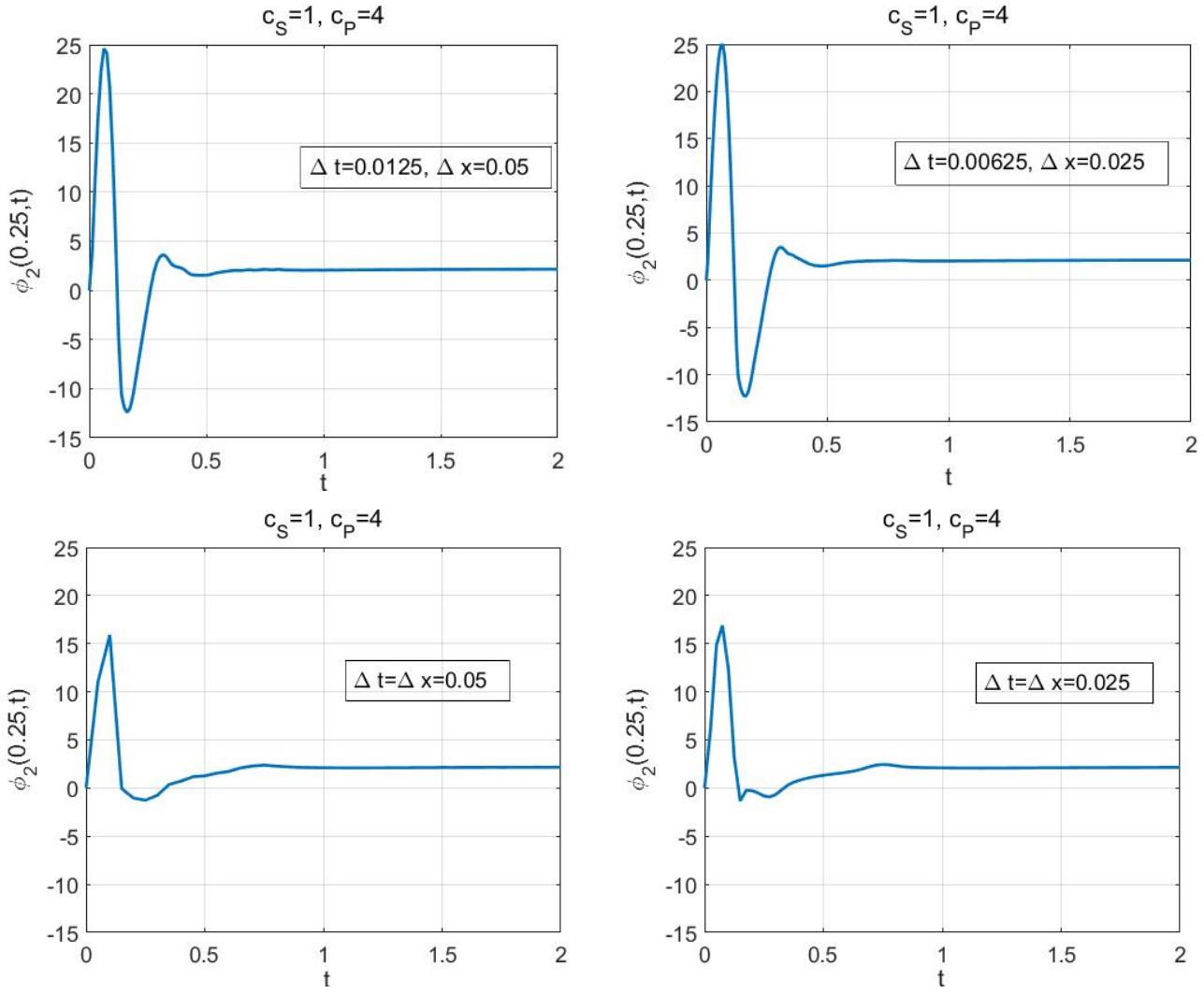

Figure 6. Vertical component $\phi_2(0.25, t)$ of the transient solution on the time interval $[0, 2]$, for different values of the discretization parameters, for $c_{\mathrm{S}} = 1$, $c_{\mathrm{P}} = 4$.

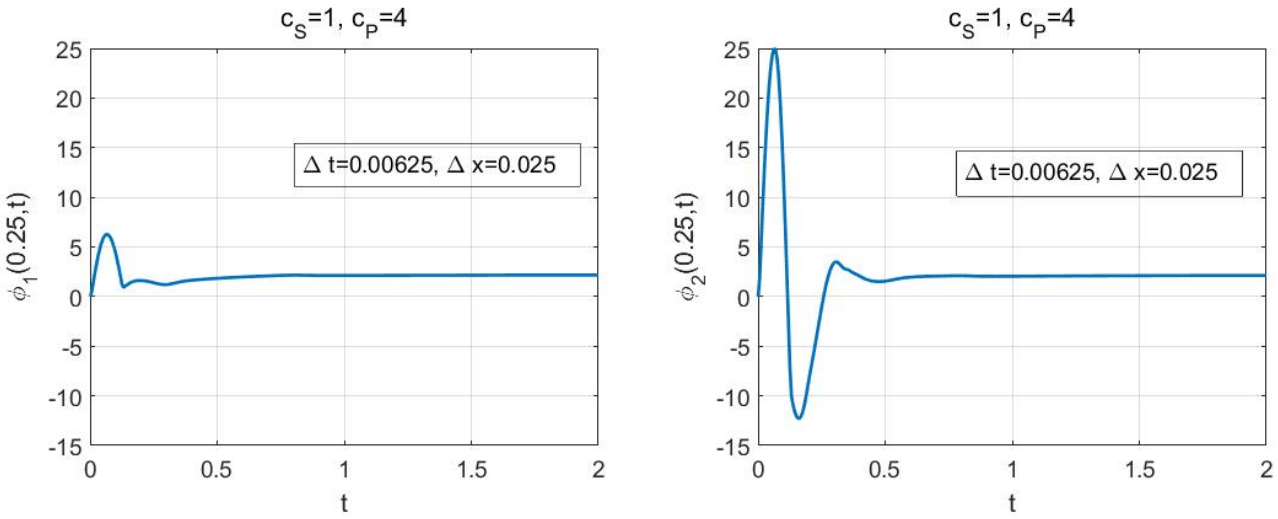

Figure 7. $\phi_i(0.25, t)$, $i = 1, 2$ evaluated by Energetic BEM, for $c_{\mathrm{S}} = 1$, $c_{\mathrm{P}} = 4$.

Table 1. Absolute errors $|\phi_2(x_1,t)-\phi_{2,\infty}(x_1)|$.

$\Delta x=0.05, \Delta t=0.025$				
	$t=4$	$t=6$	$t=8$	$t=10$
$x_1=0$	$6.3868\,10^{-4}$	$1.1154\,10^{-3}$	$1.2774\,10^{-3}$	$1.3505\,10^{-3}$
$x_1=0.1$	$3.6059\,10^{-3}$	$6.0683\,10^{-3}$	$6.9043\,10^{-3}$	$7.2815\,10^{-3}$
$x_1=0.2$	$8.2633\,10^{-3}$	$1.3082\,10^{-2}$	$1.4717\,10^{-2}$	$1.5454\,10^{-2}$
$x_1=0.3$	$1.5890\,10^{-3}$	$9.7574\,10^{-3}$	$1.2523\,10^{-2}$	$1.3770\,10^{-2}$
$x_1=0.4$	$7.8530\,10^{-1}$	$7.7219\,10^{-1}$	$7.6776\,10^{-1}$	$7.6576\,10^{-1}$
$\Delta x=0.025, \Delta t=0.0125$				
	$t=4$	$t=6$	$t=8$	$t=10$
$x_1=0$	$3.8036\,10^{-6}$	$2.3543\,10^{-4}$	$3.1679\,10^{-4}$	$3.5353\,10^{-4}$
$x_1=0.1$	$1.3757\,10^{-4}$	$2.3486\,10^{-3}$	$3.1004\,10^{-3}$	$3.4398\,10^{-3}$
$x_1=0.2$	$1.3562\,10^{-3}$	$5.8631\,10^{-3}$	$7.3941\,10^{-3}$	$8.0852\,10^{-3}$
$x_1=0.3$	$6.4774\,10^{-3}$	$1.4198\,10^{-2}$	$1.6817\,10^{-2}$	$1.7998\,10^{-2}$
$x_1=0.4$	$4.4951\,10^{-3}$	$1.8608\,10^{-2}$	$2.3385\,10^{-2}$	$2.5539\,10^{-2}$
$\Delta x=0.0125, \Delta t=0.00625$				
	$t=4$	$t=6$	$t=8$	$t=10$
$x_1=0$	$1.0083\,10^{-4}$	$1.8926\,10^{-5}$	$5.9689\,10^{-5}$	$7.8103\,10^{-5}$
$x_1=0.1$	$1.6715\,10^{-3}$	$4.1334\,10^{-4}$	$1.1228\,10^{-3}$	$1.4432\,10^{-3}$
$x_1=0.2$	$2.9109\,10^{-3}$	$1.4396\,10^{-3}$	$2.9187\,10^{-3}$	$3.5865\,10^{-3}$
$x_1=0.3$	$2.6140\,10^{-3}$	$4.8590\,10^{-3}$	$7.3962\,10^{-3}$	$8.5410\,10^{-3}$
$x_1=0.4$	$8.0229\,10^{-3}$	$2.1557\,10^{-2}$	$2.6143\,10^{-2}$	$2.8211\,10^{-2}$

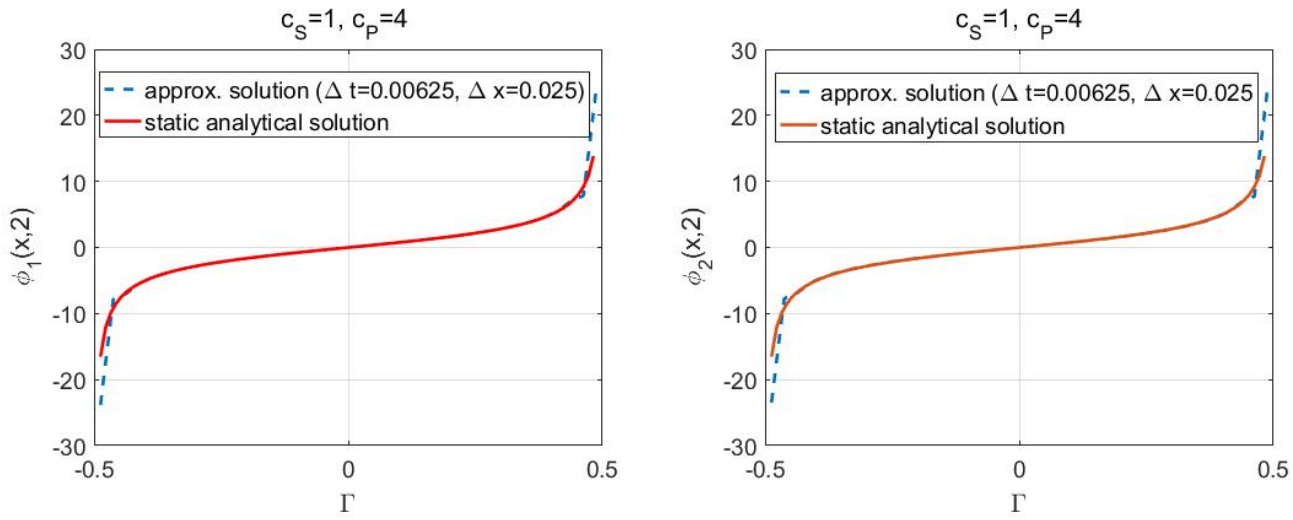

Figure 8. $\phi_i(x_1,2)$ compared to $\phi_{i,\infty}(x_1)$, $i=1,2$, for $c_S=1$, $c_P=4$.

Acknowledgements

This work has been partially supported by INdAM, Italy, through granted GNCS research projects.

$$\bar{u}_2(\cdot,t) = \begin{cases} t-\frac{1}{2}\,, & t\in[0.5,0.6] \\ \frac{-30\,t+19}{10}\,, & t\in[0.6,0.7] \\ \frac{40\,t-30}{10}\,, & t\in[0.7,0.8] \\ \frac{-30\,t+26}{10}\,, & t\in[0.8,0.9] \\ t-1\,, & t\in[0.9,1] \\ 0 & \text{elsewhere} \end{cases}$$

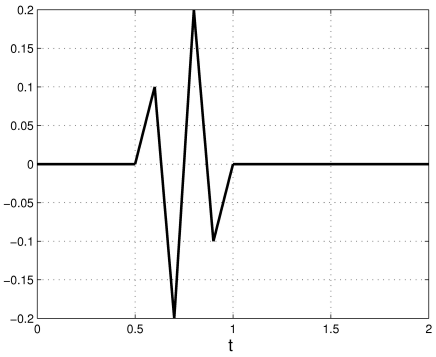

Figure 9. Dirichlet boundary condition.

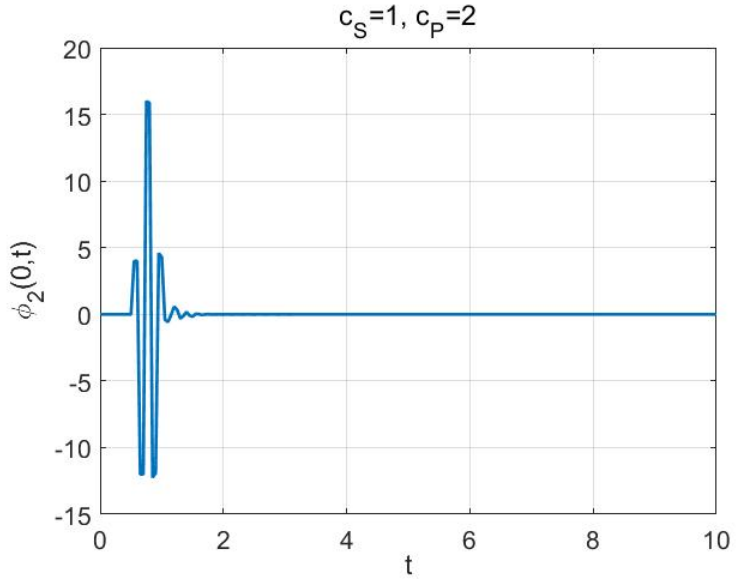

Figure 10. Density $\phi_2(0,t)$, obtained for $\Delta t = 0.05$ and $\Delta x = 0.1$.

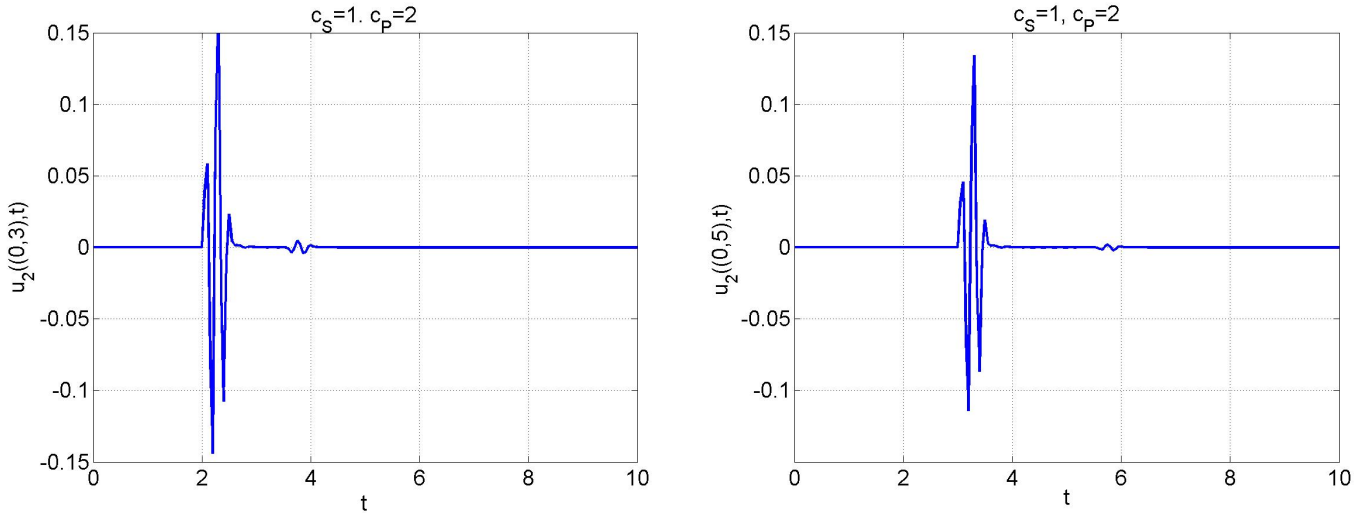

Figure 11. Vertical displacement $u_2(\mathbf{x},t)$ in $\mathbf{x}=(0,3)$ (left) and $\mathbf{x}=(0,5)$ (right), obtained for $\Delta t = 0.05$ and $\Delta x = 0.1$.

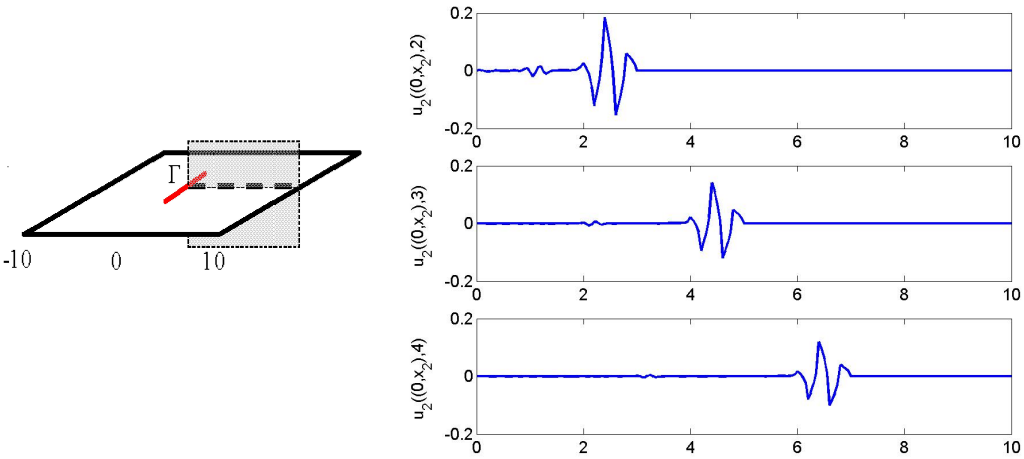

Figure 12. Section of $u_2(\mathbf{x}, t)$ along $x_1 = 0$, $0 < x_2 < 10$, at time instants $t = 2, 3, 4$.

References

1. P. Banerjee, *The boundary element in engineering (2nd. edition)*. McGraw-Hill, U.K. Ltd., 1994.
2. D. Beskos, Boundary Element methods in Dynamic Analysis, *App. Mech. Rev.*, vol. 4, no. 1, pp. 1–23, 1987.
3. M. Costabel, Time-dependent problems with the boundary integral equation method, in *Encyclopedia of Computational Mechanics* (E. S. et al., ed.), pp. 1–28, John Wiley and Sons, 2004.
4. T. Cruse and F. Rizzo, A direct formulation and numerical solution of the general transient elastodynamic problem. I, *Journal of Mathematical Analysis and Applications*, vol. 22, pp. 244–259, 1968.
5. J. Dominguez, Boundary element methods in dynamic analysis, *Applied Mechanical Engineering*, vol. 4, pp. 1–23, 1987.
6. S. Chaillat, L. Desiderio, and P. Ciarlet, Theory and implementation of H-matrix based iterative and direct solvers for Helmholtz and elastodynamic oscillatory kernels, *Journal of Computational Physics*, vol. 351, pp. 165–186, 2017.
7. L. Desiderio, An H-matrix based direct solver for the boundary element method in 3D elastodynamics, *AIP Conference Proceedings*, vol. 1978, 2018.
8. H. Antes, A boundary element procedure for transient wave propagations in two-dimensional isotropic elastic media, *Finite Elements Analysis and Design*, vol. 1, pp. 313–321, 1985.
9. D. Cole, D. Kosloff, and J. Minster, A numerical boundary integral equation method for elastodynamics, *Bulletin of the Seismological Society of America*, vol. 68, pp. 1331–1357, 1978.
10. G. Maier, M. Diligenti, and A. Carini, A variational approch to boundary element method elastodynamic analysis and extension to multidomain problems, *Computer Methods in Applied Mechanics and Engineering*, vol. 92, pp. 193–213, 1991.
11. W. Mansur and C. Brebbia, Numerical implementation of boundary element method for two-dimensional transient scalar wave propagation problems, *Applied Mathematical Modelling*, vol. 6, pp. 299–306, 1982.
12. E. Becache, A variational boundary integral equation method for an elastodynamic antiplane crack, *International Journal for Numerical Metods in Engineering*, vol. 36, pp. 969–984, 1993.
13. A. Bamberger and T. Ha Duong, Formulation variationelle espace-temps pour le calcul par potential retardé de la diffraction d'une onde acoustique (I), *Mathematical Methods in the Applied Sciences*, vol. 8, pp. 405–435, 1986.
14. A. Bamberger and T. Ha Duong, Formulation variationelle pour le calcul de la diffraction d'une onde

acoustique par une surface rigide, *Mathematical Methods in the Applied Sciences*, vol. 8, pp. 598–608, 1986.

15. T. Ha Duong, On retarded potential boundary integral equations and their discretization, in *Topics in computational wave propagation. Direct and inverse problems* (P. Davies, ed.), pp. 301–336, Springer-Verlag, 2003.
16. T. Ha Duong, On the transient acoustic scattering by a flat object, *Japan Journal of Industrial and Applied Mathematics*, vol. 7, pp. 489–513, 1990.
17. C. Lubich, Convolution quadrature and discretized operational calculus. I, *Numerische Mathematik*, vol. 52, pp. 129–145, 1988.
18. C. Lubich, Convolution quadrature and discretized operational calculus. II, *Numerische Mathematik*, vol. 52, pp. 413–425, 1988.
19. C. Lubich, On the multistep time discretization of linear initial-boundary value problems and their boundary integral equations, *Numerische Mathematik*, vol. 67, pp. 365–389, 1994.
20. A. Aimi and M. Diligenti, A new space-time energetic formulation for wave propagation analysis in layered media by BEMs, *International Journal for Numerical Methods in Engineering*, vol. 75, pp. 1102–1132, 2008.
21. A. Aimi, M. Diligenti, C. Guardasoni, I. Mazzieri, and S. Panizzi, An energy approach to space-time Galerkin BEM for wave propagation problems, *International Journal for Numerical Methods in Engineering*, vol. 80, no. 9, pp. 1196–1240, 2009.
22. A. Aimi, M. Diligenti, and S. Panizzi, Energetic Galerkin BEM for wave propagation Neumann exterior problems, *Computer Modeling in Engineering & Sciences*, vol. 58(2), pp. 185–219, 2010.
23. A. Aimi, M. Diligenti, and C. Guardasoni, On the energetic Galerkin boundary element method applied to interior wave propagation problems, *Journal of Computational Applied Mathematics*, vol. 235, pp. 1746–1754, 2011.
24. A. Aimi, M. Diligenti, A. Frangi, and C. Guardasoni, A stable 3D energetic Galerkin BEM approach for wave propagation interior problems, *Engineering Analysis with Boundary Elements*, vol. 36, pp. 1756–1765, 2012.
25. A. Aimi, M. Diligenti, A. Frangi, and C. Guardasoni, Neumann exterior wave propagation problems: computational aspects of 3D energetic Galerkin BEM, *Computational Mechanics*, vol. 51, pp. 475–493, 2013.
26. A. Aimi, M. Diligenti, and C. Guardasoni, Energetic BEM for the numerical analysis of 2D Dirichlet damped wave propagation exterior problems, *Communications in Applied and Industrial Mathematics*, vol. 8, pp. 103–127, 2017.
27. A. Aimi, M. Diligenti, and C. Guardasoni, Energetic BEM for the numerical solution of 2D hard scattering problems of damped waves by open arcs, in *Structured Matrices in Numerical Linear Algebra - Analysis, Algorithms and Applications* (D. Bini, F. Di Benedetto, E. Tyrtyshnikov, and M. Van Barel, eds.), vol. 30 of *Springer INdAM Series*, pp. 267–283, 2019.
28. A. Aimi, M. Diligenti, and C. Guardasoni, Comparison between numerical methods applied to damped wave equation, *Journal of Integral Equations and Applications*, vol. 29(1), pp. 5–40, 2017.
29. E. Stephan and M. Suri, On the convergence of the p-version of the Boundary Element Galerkin Method, *Math. Comp.*, vol. 52, no. 185, pp. 31–48, 1989.
30. A. Aimi and S. Panizzi, BEM-FEM coupling for the 1D Klein–Gordon equation, *Numer. Methods Partial. Diff. Eq.*, vol. 30, pp. 2042–2082, 2014.
31. A. Aimi, L. Desiderio, M. Diligenti, and C. Guardasoni, A numerical study of energetic BEM-FEM applied to wave propagation in 2D multidomains, *Publications de l'Institut Mathématique*, vol. 96, no. 110, pp. 5–22, 2014.
32. A. Aimi, M. Diligenti, A. Frangi, and C. Guardasoni, Energetic BEM-FEM coupling for wave propagation in 3D multidomains, *International Journal for Numerical Methods in Engineering*, vol. 97, pp. 377–394, 2014.
33. F. Postell and E. Stephan, On the h-, p- and h-p versions of the boundary element method - Numerical

results, *Comput. Methods Appl. Mech. Engrg.*, vol. 83, pp. 69–89, 1990.

34. A. Aimi, M. Diligenti, and G. Monegato, New numerical integration schemes for applications of Galerkin BEM to 2-D problems, *Int. J. Num. Meth. Engng.*, vol. 40, pp. 1977–1999, 1997.